Transactions on Machine Intelligence 3(3) (2020) 136-148

ISSN Online: 2821-1693

Transactions on Machine Intelligence

Journal Homepage: https://tmachineintelligence.ir/index.php/TMI

A New Approach in Designing Electrostatic Energy Harvesters with Precise Modeling of Capacitors in 3D Interdigitated Electrode Structures Considering Full Edge Capacitance Effects

M. Jahangiri[1], J. Yavand Hasani[2,*]

[1] MSc Student, Department of Electronics, School of Electrical Engineering, Iran University of Science and Technology, Tehran, Iran

[2] Assistant Professor, Department of Electronics, School of Electrical Engineering, Iran University of Science and Technology, Tehran, Iran

ARTICLE INFO

Article History:
Received 3 May 2020
Received in revised form 8 July 2020
Accepted 2 September 2020
Available online 3 September 2020

Keywords:
Optimization, Electrostatic Energy Harvester, 3D Interdigitated Electrodes, Fixed Voltage

ABSTRACT

The analysis and mathematical modeling of energy harvesting structures facilitate the optimal design of these generators. The capacitive effect between two metal plates in an energy harvester plays a crucial role in its performance. Therefore, mathematically modeling this capacitive effect is essential for the design, performance analysis, and optimization of these generators. In fixed-voltage energy harvesters, interdigitated electrode structures are used. This paper first presents novel closed-form mathematical relations to calculate the capacitive effect in energy harvesters with interdigitated structures. Then, using the derived formulas, a new approach to optimizing the structure and dimensions of these harvesters is provided. The obtained formula for modeling the capacitor in interdigitated structures is highly accurate, considers the 3D structure, and includes the effect of the number of electrodes. The aim of optimizing the target harvester structure is to maximize the harvested energy for a given dimension. The mathematical relations presented for calculating capacitive effects are initially validated using COMSOL and MATLAB software, demonstrating their high accuracy. Ultimately, the proposed optimization approach yields a 23% increase in output power compared to reported references.

1. INTRODUCTION

With the growth of microelectromechanical systems (MEMS) and the need for energy harvesting, extensive research has been conducted on energy harvesting systems, especially electrostatic systems [1-5]. The optimization of fixed-voltage energy harvesters is particularly significant because these types of harvesters are highly compatible with MEMS and CMOS technologies, are highly compact, and have suitable efficiency in small sizes. These harvesters utilize the capacitive effect between two metal plates to convert mechanical energy into electrical energy. Electrostatic energy harvesters are based on variable capacitors, typically achieved by keeping one plate fixed while

* Corresponding Author: yavand@iust.ac.ir
Department of Electronics, School of Electrical Engineering, Iran University of Science and Technology, Tehran, Iran

http://dx.doi.org/10.47176/TMI.2020.136

the other plate is attached to a moving element [6]. Electrostatic energy harvesters can be divided into two categories: (1) using an external voltage source; (2) using electrets. The first method employs an external power supply to create an electric potential difference (electric field flux) between two parallel plates, further divided into constant-voltage and constant-charge methods.

In this paper, we used a constant-voltage system because these systems can produce more energy than constant-charge systems and are simpler and less costly to fabricate compared to electret-based generators [7]. The structure used in this paper is of the in-plane type with varying overlapping regions and interdigitated electrodes. Its advantage over varying gap generators is that it is easier to control, and the system is less susceptible to damage from sudden vibrations as the electrodes move horizontally, preventing adhesion issues. Additionally, in-plane generators produce more energy due to higher energy density, and interdigitated structures allow greater capacitive changes, leading to more energy and power [7].

The change in capacitance is achieved by varying the distance or the overlapping area between the plates, making accurate capacitance calculation critical in these harvesters [8]. Accurate capacitive effect calculation is vital in many applications, including MEMS device modeling, semiconductor device modeling, sensors, and transmission line modeling [9]. Accurate capacitance calculation in various structures requires modeling the fringe capacitance effects, resulting from the electric field spreading around the electrodes, creating multiple capacitive effects around the metal plates.

Chang et al. provided a formula for calculating fringe capacitance using a two-step Conformal Mapping method, which, although very precise with only 1% deviation from Comsol results, was quite complex. Their analysis was for a very simple structure, and no formula was provided for interdigitated structures [10]. Sakura and Tamaru presented a numerical formula for fringe capacitance in 3D structures, which, despite being an improvement, deviated 6% from Comsol simulations. Their method was numerical without a comprehensive solution, and they only analyzed simple one, two, and three-line structures without providing a formula for interdigitated structures [11]. Yu Feng et al. presented a model for fringe capacitance when electrodes are fully overlapped, deriving a 3D formula for maximum capacitance without providing a minimum capacitance formula, and their analyzed structure was simple [12]. Aditya Bansal et al. provided a model for fringe capacitance when electrodes have no overlap, achieving good accuracy and a comprehensive solution for minimum capacitance, but their structure was physically simple and analyzed only in 2D [6].

Previous works used Conformal Mapping methods for 2D structures with only two facing electrodes, not analyzing 3D structures with interdigitated electrodes. In this paper, we modified the relations obtained in reference [6] to model 3D capacitance for interdigitated structures. The method used is based on Conformal Mapping. This paper presents a simpler and more accurate formula for calculating capacitance with fringe effects in a more complex 3D structure compared to those analyzed in the literature. The derived results are compared with Comsol Multiphysics numerical FEM technique simulations, showing high accuracy. After obtaining the above formulas, we used them to optimize the structure of a 3D energy harvester with interdigitated electrodes. Our results indicate a 23% increase in energy production with the optimization.

2. STRUCTURE AND ANALYSIS OF ELECTROSTATIC ENERGY HARVESTERS

Fixed-voltage energy harvesters consist of two facing metal plates, where changing the gap or overlapping area between the plates alters the capacitive effect. The periodic movement of the plates results in a minimum (C_{min}) and maximum (C_{max}) capacitive value. Since the output power of these harvesters depends on the capacitance in maximum and minimum states, C_{max} and C_{min} are significant. Simple energy harvesters typically use an external voltage source. Figure 1 shows the circuit model for an electrostatic energy harvester. As observed, the circuit includes two switches, a variable capacitor, and a load (resistor) [13].

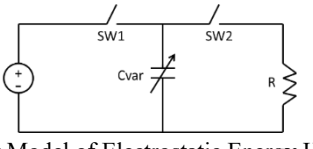

Fig.1. Circuit Model of Electrostatic Energy Harvester [13]

Figure 2 shows the charge-voltage (Q-V) diagram for the electrostatic conversion cycle with an external voltage source. The 1-2-3-1 cycle represents an energy conversion cycle with a constant voltage. This cycle starts with a constant voltage when the two plates are in complete overlap and the capacitor is at its maximum capacity (C_{max}) (path 1-2), while connected to an external voltage source. Then, with applied vibrations, the upper plate starts to move, reducing the capacitance from C_{max} to C_{min} while the capacitor remains connected to the voltage source (path 2-3). Consequently, the charge in the energy harvester structure decreases, and the structure is disconnected from the voltage source, sending the electric charge to the external load (resistor). At this stage, mechanical energy is converted into electrical energy. This operation requires two switches synchronized with the mechanical vibration. Switch SW1 closes during the initial period (path 1-2), and switch SW2 closes during the discharge period (path 3-1) [13]. When reaching C_{min}, the voltage source is removed from the circuit. Along path 3-1, the switch disconnects the generator from the source, the capacitance increases, and the charge returns to its initial value, recovering the remaining charge in the capacitor [14].

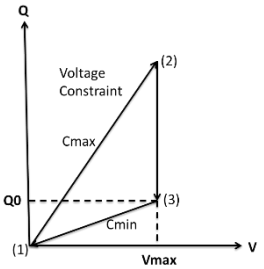

Fig.2. Electrostatic Conversion Cycle with External Voltage Source [14]

The energy obtained in each cycle is given by [13]:

$$E = \frac{1}{2} V_{in}{}^{2} (C \frac{C_{max}}{C_{min)\ (1)}} min_{max} \quad (1)$$

where V_{in}, C_{max}, and C_{min} are the initial voltage, maximum capacitance, and minimum capacitance, respectively.

It is observed that the amount of energy harvested in each cycle is proportional to $^{Cmax}/_{Cmin}$ and $C_{max} - C_{min}$. Therefore, having accurate mathematical relations to calculate these capacitances is crucial for the mathematical analysis and optimization of this energy harvester structure.

3. MODELING THE CAPACITANCE EFFECT IN FIXED VOLTAGE ENERGY HARVESTERS

The goal of this section is to present some relations mentioned in references for calculating the capacitance effect in fixed voltage energy harvesting structures or similar structures. Since the relations in this paper are developed based on the aforementioned formulas, we present these formulas in this section.

In a simple non-interdigitated structure shown in Figure 3, two overlapping electrodes face each other. The simplest available formula for calculating the capacitance effect in the structure of Figure 3 is the well-known relation:

$$C_{pp} = \frac{A(t)\varepsilon_0}{d} \quad (2)$$

where ε_0, $A(t)$, and dare the dielectric permittivity, the overlapping area between the two electrodes, and the distance between the two electrodes, respectively.

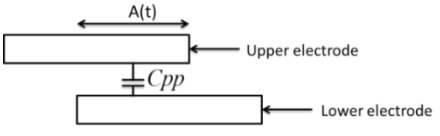

Fig.3. Structure of Two Opposing Electrodes (Non-interdigitated)

Equation (2) has very low accuracy in modeling fixed voltage energy harvesters with interdigitated structures because, in this structure, the overlapping area of the plates varies from 0% to 100%, and the Fringe field effect is significant. On the other hand, various methods have been proposed for calculating the Fringe effect, most of which are very complex [10]. Therefore, we have developed our analysis relations based on the precise yet relatively simple formulas obtained in references [6] and [12] using the Conformal Mapping method. In reference [1], the total capacitance effect between two non-overlapping parallel plates in a two-dimensional space is divided into different components, each calculated separately. These components are shown in Figure 4.

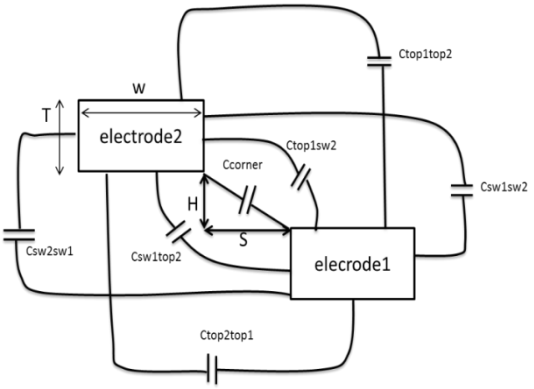

Fig.4. Types of Capacitance Between Two Non-overlapping Parallel Electrodes [6]

In this figure, the variables are: ε_{di}, the dielectric permittivity; W, the width of the electrode; T, the thickness of the electrode; s, the horizontal distance between the two electrodes; and H, the vertical distance between the two electrodes. According to reference [6], the capacitances in Figure 4 are calculated as follows:

$$C_{\text{swtop}} = \frac{\varepsilon_{di}}{(\pi/2)} ln[\frac{H+\eta T+\sqrt{2H\eta T+(\eta T)^2+S^2}}{S+H}] \quad (3)$$

According to reference [6] and using the Conformal Mapping method, the Fringe capacitance is ultimately obtained as:

$$C_{\text{fr}} = C_{corner} + \left(C_{sw2top1} + C_{sw1top2}\right) + \left(C_{top2top1} + C_{top1top2}\right) + (C_{sw1sw2} + C_{sw2sw1}) \quad (4)$$

where $\left(C_{sw2top1} = C_{sw1top2}\right), \left(C_{top2top1} = C_{top1top2}\right), (C_{sw1sw2} = C_{sw2sw1})$ are as previously defined.

In general, the total capacitance is given by $C = C_{pp} + C_{fr}$, where C_{pp} is the parallel plate capacitance and C_{fr} is the Fringe effect capacitance. It should be noted that when the electrodes are in full overlap, the capacitance is at its maximum, and as seen in Figure 4, C_{corner} does not exist. Thus, in the overall formula, the related term is removed, and the remaining capacitances in equation (4) are retained. In this state, the capacitance resulting from the full overlap of the electrodesc_{pp} (is added to the maximum capacitance. Ultimately, for maximum and minimum capacitance, we have:

$$C_{\ corner}\left(C_{sw2top1} + C_{sw1top2}\right)\left(C_{top2top1} + C_{top1top2}\right)(C_{sw1sw2} + C_{sw2sw1})_{min} \quad (5)$$

$$C_{max} = [\left(C_{sw2top1} + C_{sw1top2}\right) + \left(C_{top2top1} + C_{top1top2}\right) + (C_{sw1sw2} + C_{sw2sw1})] + [\ C_{pp}] \quad (6)$$

In reference [12], for a structure with only two fully overlapping opposing electrodes, the maximum capacitance is calculated, providing a formula for two fully overlapping electrodes in a three-dimensional state. Ultimately, based on this, we have for maximum capacitance:

$$C_{max} = \frac{LW\varepsilon_{di}}{H} + \frac{\pi\varepsilon_{di}\,(L+W)}{\ln[\left(\frac{\pi}{2}\left(1+\frac{H}{T}\right)\right)+\sqrt{\frac{\pi^2}{4}\left(1+\frac{H}{T}\right)^2-1)]}} \quad (7)$$

where W, L, H, T, and ε_{di} are the width of the electrode, the length of the electrode, the air gap between the upper and lower electrodes, the height of the electrode, and the dielectric permittivity, respectively [12].

4. PROPOSAL OF A 3D STRUCTURE WITH INTERDIGITATED ELECTRODES AND NEW MATHEMATICAL MODEL

Figure 5 shows a 3D view of the interdigitated electrodes. In Figure 5, the variables are: T for electrode thickness, W for electrode width, L for electrode length, e for the distance between two electrodes, n for the number of electrodes, and H for the air gap.

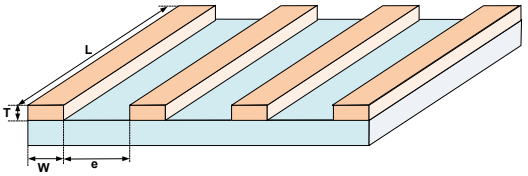

Fig.5. Variables of the 3D Electrode Structure

In the maximum capacitance state, two electrodes are fully aligned, and in the minimum capacitance state, two electrodes have no overlap (A(t) = 0). In this state, according to the formula, the capacitance becomes zero. However, in reality, this is not the case, and due to the presence of the Fringe effect, the capacitance does not become zero, indicating the necessity of considering this effect. Figure 6 shows the electric fields around the electrodes in an energy harvester with interdigitated electrodes when the electrodes have no overlap, and the Fringing effect is predominant [15].

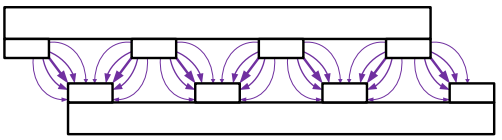

Fig.6. Electric Fields Around Interdigitated Electrodes in Minimum Capacitance State

In the case of interdigitated electrodes, the effect of fringe capacitance increases. Reference [11] provides a relationship for calculating the total capacitance for interdigitated structures (Figure 5). The provided equation is:

$$C(x) = \left(\frac{C_{max}+C_{min}}{2}\right) + \left(\frac{C_{max}-C_{min}}{2}\right)\cos\frac{2\pi x}{W+e} \quad (8)$$

In equation (8), the capacitance values at maximum and minimum states are of particular importance. These two capacitances are highly dependent on the dimensions of the structure [11]. Three main variables influencing these capacitances namely, W, e, and n, which represent the width of the electrodes, the distance between adjacent electrodes, and the number of electrodes, respectively (Figure 5)—are examined.

To model the fringe effect and derive a formula corresponding to this effect, it is sufficient to accurately model and measure the capacitance values at maximum and minimum states. Using equation (8), the total capacitance for 3D interdigitated structures can be obtained, as existing formulas lack the accuracy needed to calculate the capacitance in maximum and minimum states. Therefore, considering equations (5) and (6) for maximum and minimum capacitance, we have:

$$C_{min} = \left[\left(C_{sw2top1} + C_{sw1top2}\right) + \left(C_{top2top1} + C_{top1top2}\right) + \left(C_{sw1sw2} + C_{sw2sw1}\right) + C_{corner}\right] \times 2n(L+W) \quad (9)$$

$$C_{max} = \left[\left(\left(C_{sw2top1} + C_{sw1top2}\right) + \left(C_{top2top1} + C_{top1top2}\right) + \left(C_{sw1sw2} + C_{sw2sw1}\right)\right).2(L+W).n\right] + \left[n.C_{pp}\right] \quad (10)$$

Equation (7) from reference [12], which is for 3D structures, needs to be multiplied by the number of electrodes n. Thus, we have:

$$C_{max} = (\frac{LW\varepsilon_{di}}{H} + \frac{\pi\varepsilon_{di}\,(L+W)}{\ln[\left(\frac{\pi}{2}\left(1+\frac{H}{T}\right)\right)+\sqrt{\frac{\pi^2}{4}\left(1+\frac{H}{T}\right)^2-1)]}})n \quad (11)$$

By comparing the obtained relationships (equations (9) and (10)) with the actual results in Comsol software, we see:

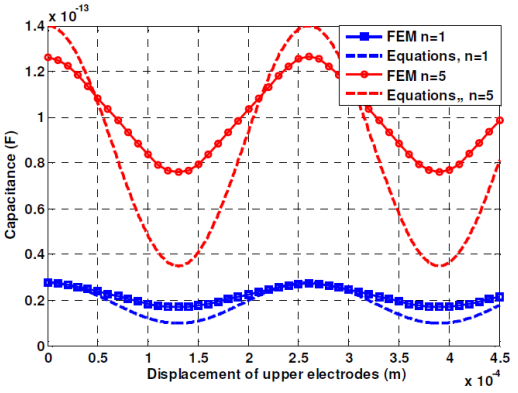

Fig.7. Comparison of Total Capacitance for Generators with Different Numbers of Electrodes, Obtained from Formula in Reference [6] Compared to Values from Comsol Software

Figure 7 shows a significant difference between the real values in Comsol software and equations (9) and (10), indicating that these relationships, especially for minimum capacitance, are inefficient. To reduce this difference, a new formula must be proposed. Comparing Figure 5 with the 2D structure used in reference [6] shown in Figure 4, it can be inferred that if W is much larger than e, the structure in Figure 5 will replicate that in Figure 4. However, if W is not large relative to e, parts of the fringe field present in Figure 4 will not exist in Figure 5. Thus, it seems that the correction term should be a function of the W/e ratio. We ultimately arrived at the following relationships:

$$C_{min}\left[\left(C_{sw2top1}+C_{sw1top2}\right)+\left(C_{top2top1}+C_{top1top2}\right)+\left(C_{sw1sw2}+C_{sw2sw1}\right)+C_{corner}\right]\times 2n(L+W)+\left[n\left(2\times 10^{(-14)}\right)\left(\frac{W}{e}\right)^{(0.8)}\right] \quad (12)$$

$$C_{max} = [\left(\left(C_{sw2top1}+C_{sw1top2}\right)+\left(C_{top2top1}+C_{top1top2}\right)+\left(C_{sw1sw2}+C_{sw2sw1}\right)\right).n^{\left(1.24-\left(\frac{w}{e}\right)\right)}.2(L+w)]+\left[n.\ C_{pp}\right] \quad (13)$$

5. COMPARISON OF COMSOL SIMULATION RESULTS WITH NEW CORRECTED FORMULAS AND VALIDATION

To evaluate the accuracy of the provided relationships and those from other articles, we used simulations in Comsol Multiphysics software. For the simulation in Comsol, all electrodes made of silicon are placed on a quartz layer, and the capacitance is obtained using the electrostatic module. An example of the structure in the Comsol software environment is shown in Figure 8.

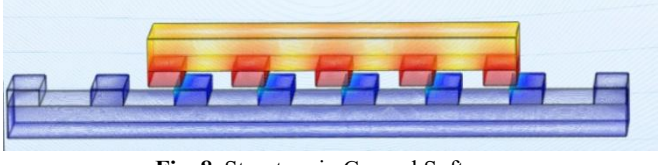

Fig. 8. Structure in Comsol Software

First, we compare the formula provided in reference [12] for calculating C_{max} with the corrected formula in this paper. For this purpose, we performed Comsol simulations with W equal to 100, T equal to 50, and varying numbers of electrodes (n). The results are shown in Table 1. The error obtained for equation (13) is very low and negligible,

making the real results very close to the new corrected formula presented in this paper. We calculated the error transparently, and in all cases, the error of our formula is less than 2%, whereas the error for equation (11) is higher.

Table 1. Comparison of C_{max} with Different Numbers of Electrodes

Variables				Total Capacitor $C_T = C_{pp} + C_{fr}(10^{-14}\text{F})$				
Number of Electrodes (n)	Electrode width (μm)	Electrode thickness (T) (μm)	C_{pp} (10^{-14}F)	Comsol	Equation (11)[12]	Equation (13) [Present Work]	Error (%)[12]	Error (%) [Present Work]
2	100	50	4.425	5.24	5.331	5.283	1.73	0.82
3	100	50	6.637	7.64	7.544	7.739	1.25	1.29
4	100	50	8.85	10	9.756	10.16	2.44	1.60
5	100	50	11.06	12.7	11.97	12.57	5.74	1.02

For a more precise evaluation of the provided formulas, we repeated the Comsol simulation with W equal to 100, T equal to 50, and varying numbers of electrodes (n), comparing the results with our derived formulas. The results are shown in Figure 9. In this figure, it is observed that the obtained results are very close to those in Comsol, providing an accurate approximation of the real situation by the new corrected formula (Equations (12) and (13)). The significance of the provided formula is better understood by comparing Figure 9 with Figure 7.

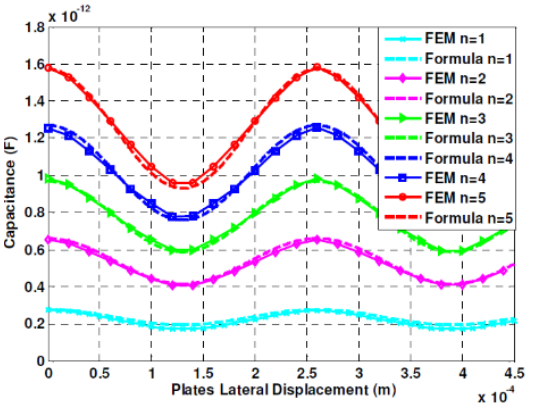

Fig. 9. Comparison of Total Capacitance of the Generator Structure Calculated by the Provided Formula with Comsol for Different Numbers of Electrodes

As previously mentioned, various variables influence the total capacitance; we have so far examined the effect of varying the number of electrodes. Two other influencing variables are the distance between adjacent electrodes (e) and the width of the electrodes (W) in the structure. Based on the provided formulas, we analyze their effects and compare them with the real situation in Comsol. In Figure 10, the number of electrodes is 5, and based on the structure's variables in Figure 5, the variables W and e range from 100 to 130 and 130 to 160 micrometers, respectively. This figure shows that the results from our model for various electrode dimensions are in good agreement with the Comsol software, indicating high accuracy.

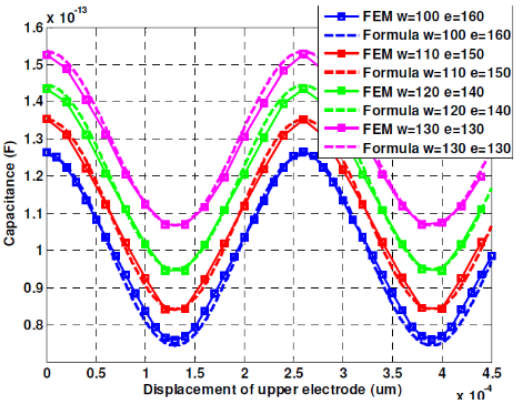

Fig.10. Comparison of Total Capacitance Obtained from the Formula Provided in This Paper with Simulation Results in Comsol for Different W and e with a Fixed Number of Electrodes n=5

In Figure 11, a comparison is made between the values of C_{max} and C_{min} using the new corrected formula in this paper (Equations (12) and (13)) and in Comsol for different numbers of electrodes. It is observed that the results from the corrected formula closely match the results in Comsol.

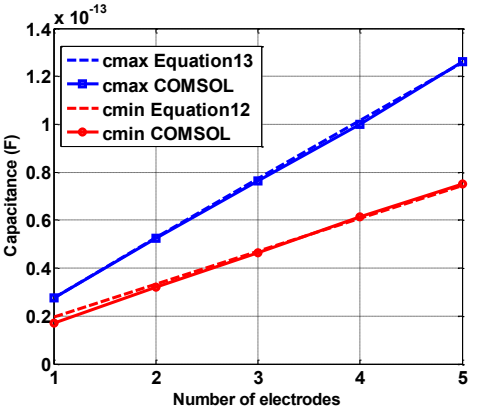

Fig.11. Comparison of C_{max} and C_{min} Using the Provided Formula and Comsol for Different Numbers of Electrodes

It should be noted that our goal in calculating the capacitances is to use them to calculate the energy per cycle for the interdigitated structure generator and ultimately employ it in the design of the generator structure. The energy per cycle is a function of C_{max} and $C_{min}$and can be mathematically calculated using equation (1). Therefore, to validate our relationships in calculating the energy per cycle, we calculated this value for generators with different numbers of electrodes, once by combining our relationships with equation (1) and again by Comsol simulation. The results are shown in Figure 12. As observed, the values obtained from the new corrected formula in this paper (Equations (12) and (13)) are very close to the real values in Comsol, while the green curve, representing the formula provided in reference [6], shows a significant difference from the real situation.

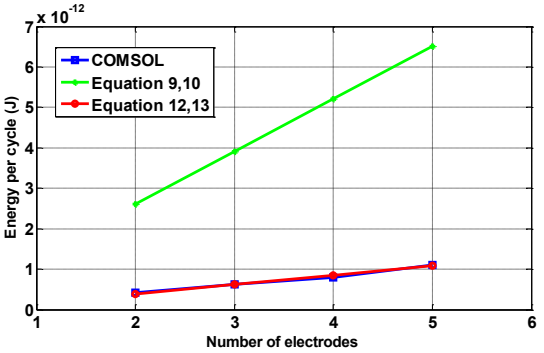

Fig.12. Comparison of Energy per Cycle Based on the Number of Electrodes in the Generator Structure, obtained from the Provided Formula, Reference [6], and Comsol Simulation

Finally, a comparison is made between the harvested energy in Comsol and the new corrected formula in this paper (equations (12) and (13)) as a function of the relative displacement of the electrodes in Figure 13. It is observed that the results obtained from the provided formula are very close to the simulated values in Comsol.

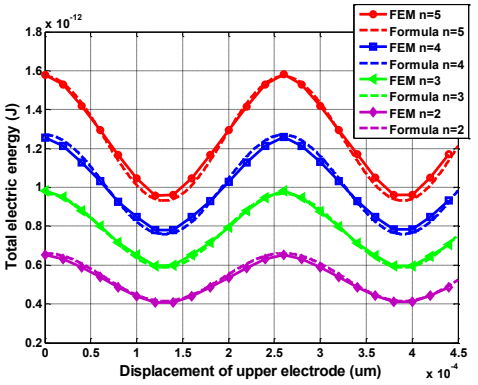

Fig.13. Comparison of Total Energy Obtained from the Provided Formula with Comsol Results as a Function of the Relative Displacement of Electrodes for Different Numbers of Electrodes

6. DIMENSION OPTIMIZATION IN ELECTROSTATIC ENERGY HARVESTERS

The goal of optimizing the generator structure is to determine the variables W (width of the electrodes) and e (distance between adjacent electrodes) such that the maximum energy is harvested with a given generator size. It is emphasized that we aim to harvest the maximum energy from a generator with specified dimensions. This optimization process is presented for the first time.

To achieve this, we use equation (1) to calculate the harvested energy per cycle. The key point in using this equation is the accurate calculation of C_{max} and C_{min}. In the previous sections, we derived precise formulas for calculating them (equations (12) and (13)). After calculating the energy harvested per cycle, it can be divided by the generator's oscillation cycle period to compute the generator's output power. The generator's structural variables are:

- Thickness of the electrodes (T)

- Width of the electrodes (W)

- Groove width, which is the distance between two adjacent electrodes (e)

- Number of electrodes (n)

In Matlab software, the harvested energy contours are plotted, and the optimal values of W and e corresponding to the maximum harvested energy are identified.

In the first step, to validate the idea, we performed the optimization process for a generator with an area of 25 mm². The harvested energy contours are shown in Figure 14, and the 3D curve of harvested energy based on W and e is shown in Figure 15. These two figures clearly indicate that optimal values for W and e exist.

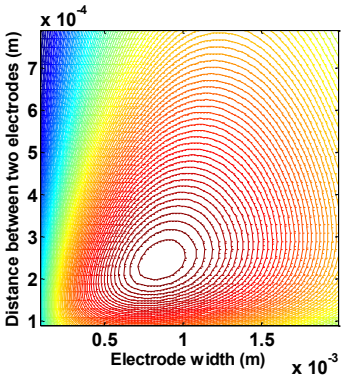

Fig.14. Contour Plot of Output Power for an Area of 25 mm² Based on Variables W and e

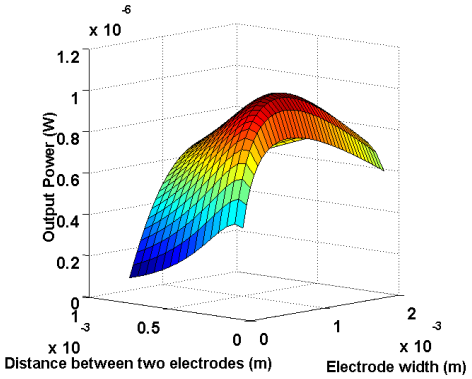

Fig.15. 3D Curve of Output Power for an Area of 25 mm² Based on Variables W and e

In Table 2, several electrostatic generators reported in recent years are reviewed, and for each, the normalized power is calculated, as shown in Table 2. Among them, the generator reported in reference [16] has the highest normalized power. This generator has an area of 1800 mm². To demonstrate the importance of the presented optimization process, we optimized a generator with the same dimensions, and the details are shown in Table 2. The harvested energy contour is shown in Figure 16, and the 3D curve of harvested energy based on W and e is shown in Figure 17. The results in Table 2 indicate that optimization increases the normalized power from 9.722*E(-5) in reference [16] to 1.203*E(-4) in this paper. This increase corresponds to a 23% improvement in the generator's performance.

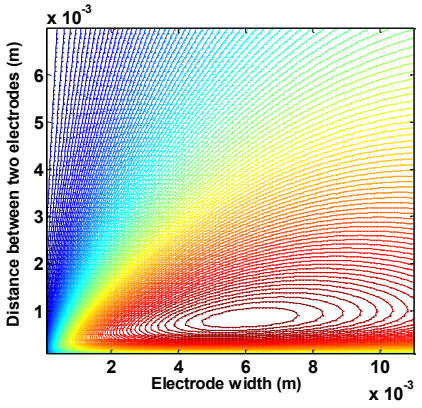

Fig.16. Contour Plots of Output Power for an Area of 1800 mm² Based on Variables W and e

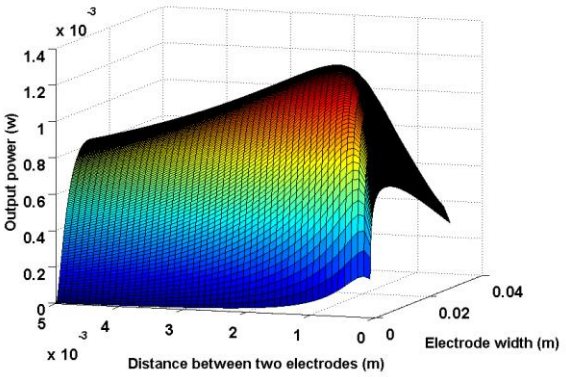

Fig.17. 3D Curve of Output Power for an Area of 1800 mm² Based on Variables W and e

Table 2. Comparison of Various Electrostatic Energy Harvesters with the Structure Presented in This Paper

Author	Ref.	Year	Functional Frequency f (Hz)	Device Area A (mm2)	Functional Voltage (V)	Output Power (uw)	Normalized Power (uw/Hz.mm².v)
Despesse *et al*	[16]	2005	50	1800	120	1050	9.722*E(-5)
Yen *et al*	[17]	2006	1560	4356	6	1.8	4.41*E(-8)
Basset *et al*	[18]	2008	250	66	8	0.061	4.62*E(-7)
Hoffmann	[19]	2008	1460	30	50	3.8	1.73*E(-6)
Mitcheson	[20]	2004	10	784	2300	24	1.33*E(-6)
Present Work	-	2020	50	1800	120	1300	1.203*E(-4)

7. CONCLUSION

We presented an optimization process for the structure of electrostatic generators with interdigitated electrode structures. In this context, we developed mathematical relationships for calculating the minimum and maximum capacitance values of the aforementioned generator structure. The formula derived in this paper is highly accurate and simple, based on formulas previously presented in references. Existing formulas are for two-dimensional and non-interdigitated structures, which we extended for three-dimensional interdigitated structures. The formulas provided in this paper are particularly suitable for applications with micro dimensions. To evaluate and validate the presented formulas, we used simulations in Comsol software, and the simulation results demonstrated high accuracy for the provided relationships.

After obtaining the closed-form mathematical relations for calculating C_{max} and C_{min}‘, we presented an optimization process for the generator structure aimed at maximizing the harvested energy per unit area of the generator. In this process, the generator's surface area is given as a design input, and the variables W (electrode width), e (electrode spacing), and n (number of electrodes) are determined using the provided process.

Finally, to demonstrate the capability and importance of this optimization process, we optimized the structure of a generator with an area of 1800 mm², which was reported in reference [16]. The simulation results showed that the harvested energy with the optimized structure is 23% higher than the amount reported in reference [16].

Transparency Statement

The data supporting this study are available upon reasonable request to the corresponding author, subject to ethical and confidentiality considerations.

Acknowledgments

We would like to express our gratitude to all individuals who contributed to this project.

Declaration of Interest

The authors declare that they have no competing interests.

Funding

This research received no specific grant from any funding agency, commercial, or not-for-profit sectors.

REFERENCES

[1] Jiang, T., Pang, H., An, J., Lu, P., Feng, Y., Liang, X., ... & Wang, Z. L. (2020). Robust swing-structured triboelectric nanogenerator for efficient blue energy harvesting. Advanced Energy Materials, 10. https://doi.org/10.1002/aenm.202000064

[2] Huang, L., Lin, S., Xu, Z., Zhou, H., Duan, J., Hu, B., & Zhou, J. (2019). Fiber-based energy conversion devices for human-body energy harvesting. Advanced Materials, 32. https://doi.org/10.1002/adma.201902034

[3] Hinchet, R., Yoon, H. J., Ryu, H., Kim, M. K., Choi, E., Kim, D. S., & Kim, S. W. (2019). Transcutaneous ultrasound energy harvesting using capacitive triboelectric technology. Science, 365, 491-494. https://doi.org/10.1126/science.aan3997

[4] Shi, Q., He, T., & Lee, C. (2019). More than energy harvesting - Combining triboelectric nanogenerator and flexible electronics technology for enabling novel micro-/nano-systems. Nano Energy. https://doi.org/10.1016/j.nanoen.2019.01.002

[5] Zhu, J., Liu, X., Shi, Q., He, T., Sun, Z., Guo, X., ... & Lee, C. (2019). Development Trends and Perspectives of Future Sensors and MEMS/NEMS. Micromachines, 11. https://doi.org/10.3390/mi11010007

[6] Bansal, A., Paul, B. C., & Roy, K. (2006). An analytical fringe capacitance model for interconnects using conformal mapping. IEEE Transactions on Computer-Aided Design of Integrated Circuits and Systems, 25(12). https://doi.org/10.1109/TCAD.2006.882489

[7] Lee, C., Lim, Y. M., Yang, B., Kotlanka, R. K., Heng, C. H., He, J. H., ... & Feng, H. (2009). Theoretical comparison of the energy harvesting capability among various electrostatic mechanisms from structure aspect. Sensors and Actuators A: Physical, 156(1), 208-216. https://doi.org/10.1016/j.sna.2009.02.024

[8] Boisseau, S., Despesse, G., & Sylvestre, A. (2010). Optimization of an electret-based energy harvester. Smart Materials and Structures, 19(7). https://doi.org/10.1088/0964-1726/19/7/075015

[9] Li, N., Zhu, H., Wang, W., & Gong, Y. (2014). Parallel double-plate capacitive proximity sensor modelling based on effective theory. AIP Advances, 4(2), 027119. https://doi.org/10.1063/1.4866986

[10] Chang, W. H. (1977). Analytical IC metal-line capacitance formulas. IEEE Trans. Microw. Theory Tech., 25. https://doi.org/10.1109/TMTT.1977.1129193

[11] Sakurai, T., & Tamaru, K. (1983). Simple formulas for two-and three-dimensional capacitances. IEEE Transactions on Electron Devices, 30(2). https://doi.org/10.1109/T-ED.1983.21093

[12] Feng, Y., Shao, B., Tang, X., Han, Y., Wu, T., & Suzuki, Y. (2018). Improved capacitance model involving fringing effects for electret-based rotational energy harvesting devices. IEEE Transactions on Electron Devices, 65(4). https://doi.org/10.1109/TED.2018.2803145

[13] Basset, P., Galayko, D., Paracha, A. M., Marty, F., Dudka, A., & Bourouina, T. (2009). A batch-fabricated and electret-free silicon electrostatic vibration energy harvester. Journal of Micromechanics and Microengineering, 19(11). https://doi.org/10.1088/0960-1317/19/11/115025

[14] Elshurafa, A. M., & El-Masry, E. I. (2007). Design considerations in MEMS parallel plate variable capacitors. In 2007 50th Midwest Symposium on Circuits and Systems (pp. 1173-1176). IEEE. https://doi.org/10.1109/MWSCAS.2007.4488764

[15] Ahmad, M. R., & Khir, M. H. B. M. (2011). Design, analysis and fabrication of Electret-based micro-electromechanical systems energy harvester. In 2011 National Postgraduate Conference (pp. 1-4). IEEE. https://doi.org/10.1109/NatPC.2011.6136424

[16] Despesse, G., Chaillout, J. J., Jager, T., Léger, J. M., Vassilev, A., Basrour, S., & Charlot, B. (2005). High damping electrostatic system for vibration energy scavenging. Proc. sOc-EUSAI 2005, 283-6. https://doi.org/10.1145/1107548.1107617

[17] Chih-Hsun Yen, B., & Lang, J. (2006). A variable capacitance vibration-to-electric energy harvester. IEEE Trans Circuits Syst., 53, 288-95. https://doi.org/10.1109/TCSI.2005.856043

[18] Basset, P., Galayko, D., Paracha, A., Marty, F., Dudka, A., & Bourouina, T. (2009). A batch-fabricated and electret-free silicon electrostatic vibration energy harvester. IOP Journal of Micromechanics and Microengineering, 19(115025). https://doi.org/10.1088/0960-1317/19/11/115025

[19] Hoffmann, D., Folkmer, B., & Manoli, Y. (2008). Fabrication and characterization of electrostatic micro-generators. Proc. PowerMEMS 2008, 15. https://doi.org/10.1088/0960-1317/19/9/094001

[20] Mitcheson, P., Green, T. C., Yeatmann, E. M., & Holmes, A. S. (2004). Architectures for vibration-driven micropower generators. J. of Microelect. Systems, 13, 429-40. https://doi.org/10.1109/JMEMS.2004.830151